

Estimation of Road Friction for Enhanced Active Safety Systems: Algebraic Approach

Changsun Ahn, Hwei Peng, and H. Eric Tseng, *Member, IEEE*

Abstract— Knowledge of tire friction force capacity, i.e. tire-load frictional coefficient, is important for the control of vehicle active safety systems. In this paper we review several methods for friction estimation and develop two robust and cost effective methods based on a nonlinear least square approach and the peak aligning torque. The methods proposed in this paper utilize simple vehicle lateral dynamics, steering system, and front tire dynamics. The first estimator uses direct calculation based on front tire self-aligning torque and the second method is based on a nonlinear least square method. These estimators are verified with Carsim under various conditions.

I. INTRODUCTION

TIRE-ROAD friction is an important characteristic that influences vehicle longitudinal, lateral/yaw and roll motions. The tire-road frictional coefficient, if accurately and timely acquired, can significantly impact the design and performance of active safety systems, because vehicle motions are predominantly affected through tire forces, governed by road friction and tire normal forces. With the exponential growth of hybrid vehicle sales, EPAS (Electric Power Assisted Steering) and AFS (Active Front Steering) could soon be widely adopted. These advanced chassis control systems, similar to ESP (Electronic Stability Program), function well only when road friction is known. When friction is not known, the control acts only based on vehicle response and the designs are usually conservative, resulting in reduced performance. In the literature many tire-road friction estimation schemes use features of tire/tread behavior (e.g., wheel speed, wheel acceleration, aligning moment, tire noise) as the basis of the estimation. For example, Eichhorn and Roth [1] used optical and noise sensor at the front-end of the tire and stress and strain sensors inside the tire's tread to study both "parameter-based" and "effect-based" road friction estimation methods. Ito *et al.* [2] used the applied traction force and the resulting wheel speed difference between driven and non-driven wheels to estimate

the road surface condition. Pal *et al.* [3] applied the neural network based identification technique to predict the road frictional coefficient based on steady-state vehicle response signals. Pasterkamp [4] developed an online estimation method based on lateral force and self-aligning torque measurements and the Delft Tire Model. Gustafsson [5] developed a model-based approach and used the difference between driven and non-driven wheels to detect tire-road friction. Liu and Peng [6] applied the special structure of the brush tire model and used wheel speed signal to estimate road frictional coefficient and cornering stiffness. These friction estimation methods identify tire-road characteristics by using longitudinal and tire dynamics, which can then be used for the adaptations of control-estimation algorithm for both lateral and longitudinal directions. Hahn [7] used lateral dynamics to estimate frictional coefficient. In particular, his algorithm relies on GPS-based vehicle lateral speed. Sierra [8] utilized lateral dynamics, including lateral speed and yaw angular acceleration to detect cornering stiffness.

Recently, Toyota published a series of papers [9]-[12] based on either measuring the self-aligning torque or lateral compliance of the rotational shaft. The experimental results presented by Umeno [12] show excellent estimation results (less than 5% error of forces up to 2500N) for both lateral force and self-aligning torque by using the measurement from a resolver mechanism. It is worthwhile to point out that the results presented in [9]-[12] do not include extreme cases, such as icy roads, high bank angle and high vehicle roll motions, which are important for assessing the performance of active safety systems. Hsu [13] introduced an algorithm to estimate frictional coefficient using nonlinear least squares. The identification method uses self-aligning torque and GPS-based sideslip measurements. He also presented a nonlinear observer using self-aligning torque and lateral acceleration in [14]. Holzmann [15] analyzed texture of images taken by camera and classified possible road types. Sato [16] and Yamada [17] measured wetness of road by detecting reflected light using optical sensors. These optical methods are effective in detecting the condition of road, but they are seriously affected by the intensity and direction of light.

In Table I, we summarized several approaches mentioned above. We ruled out the vision based, the tire force measurement based, and the tire tread based methods considering cost and technical issues. The wheel motion based method was also ruled out because of its weakness to high frequency disturbances. We excluded the lateral model

Manuscript received September 14, 2008. This work was supported by Ford Motor Company.

C. Ahn is with the Department of Mechanical Engineering, University of Michigan, Ann Arbor, MI 48109, USA (phone: 734-647-9732; e-mail: sunahn@umich.edu).

H. Peng is a professor of the Department of Mechanical Engineering, University of Michigan, Ann Arbor, MI 48109, USA (e-mail: hpeng@umich.edu).

H. E. Tseng is a technical leader of the Powertrain Controls Research & Advanced Engineering, Ford Motor Company, Dearborn, MI 48121 USA (e-mail: htseng@ford.com).

TABLE I
COMPARISON OF SEVERAL ESTIMATION APPROACHES

Category	Special sensors	Non-measurable Signal	Method to get the Signal	Sensor reliability	Vulnerability	Output	Cost	Reference
Vision based	Optical Sensors				<i>Snow/Ice</i>	<i>Qualitative</i>	<i>High</i>	[1], [15]-[17]
Tire force measurement	Force Sensors					Quantitative	<i>High</i>	[4]
Tire tread based	Stress/Strain Sensors					Quantitative	<i>High</i>	[1]
Wheel motion based					<i>High freq. disturbance</i>	Quantitative		[2], [5], [6]
Vehicle Motion (Dynamic Model)	D-GPS	V	Measured with GPS	<i>Weak to obstruction</i>		Quantitative	<i>High</i>	[7], [13]
Vehicle Motion (Fuzzy Model)		V	<i>No</i>			Quantitative		[3]
Vehicle motion only (Dynamic Model)		v \dot{r}	Estimation <i>No</i>			Quantitative		[8]
Vehicle Motion (Vehicle + Steering)		α	Estimation			Quantitative		[14]

v : vehicle lateral speed, \dot{r} : Yaw acceleration, α : tire slip angle, The critical disadvantages of each approach are highlighted.

based method with GPS sensors because of high cost. We eliminated the fuzzy model based and the vehicle model only based methods due to the limitation of excitation and difficulties in achieving required signals. We decided to use vehicle dynamics and steering dynamics for frictional coefficient estimation because the information is readily available if the vehicle has ESP and EPAS or AFS.

Estimation methods based on vehicle motion are fundamentally more robust compared with those using tire behaviors because a tire has smaller inertia and its behavior is influenced by road roughness, ABS operation, tire pressure and tread variations, tire carcass non-uniformities, and vehicle roll/pitch/vertical motions. Therefore, tire motion tends to be much more oscillatory and contain higher frequency components. Separating the effects of these disturbances from those of tire-road friction is difficult. Another benefit of using lateral/yaw dynamics for frictional coefficient estimation is that the related signals (such as steering angle, yaw rate, lateral acceleration and vehicle forward speed) are readily measured for other purposes. Therefore, incremental hardware cost is low. We suggest a robust and cost-effective vehicle lateral/yaw based estimation algorithm in this paper.

II. SYSTEM MODELS

A. Vehicle Model

The basis of our estimation methods is the bicycle vehicle model, which describes the vehicle lateral and yaw dynamics of a two-axle, one-rigid body ground vehicle, represented in Fig. 1. Assuming pure lateral slip, derivation of the equations of motion for the bicycle model follows from the force and moment balance:

$$\begin{aligned} m(\dot{v} + ur) &= F_{yf} + F_{yr}, \\ I_z \dot{r} &= aF_{yf} - bF_{yr}, \end{aligned} \quad (1)$$

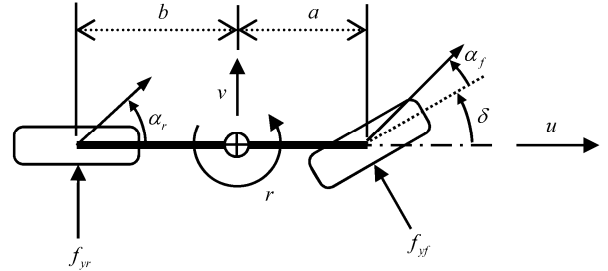


Fig. 1. Vehicle bicycle model.

where u is the vehicle forward speed, v is the vehicle lateral speed, r is the yaw rate, m is the vehicle mass, I_z is the yaw moment of inertia. F_{yf} and F_{yr} are the lateral forces at the front and rear axles, respectively. δ is the front wheel steering angle, and a and b are the distance from vehicle center of gravity to front and rear axles. Using small angle approximations, the slip angles α_f and α_r of front and rear tires in terms of u , v , and r are:

$$\begin{aligned} \alpha_f &= (v + ar) / u - \delta, \\ \alpha_r &= (v - br) / u. \end{aligned} \quad (2)$$

B. Tire Model

Under pure-slip conditions, the lateral force and self-aligning torque generated between the tires and the road are nonlinear functions of the tire slip angle. As shown in Fig. 2, tire lateral force increases linearly initially, and, eventually the force reaches saturation due to the limited friction potential between the tire and road. Tire aligning torque also shows a linear relationship to tire slip angle when the slip angle is small. Then it reaches a peak and goes down to zero as tire slip angle increases, because the pneumatic trail decreases whereas tire lateral force increases as the tire slip

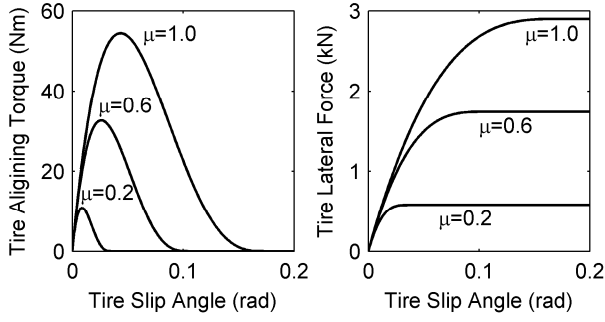


Fig. 2. Characteristics of simple tire brush model.

angle increases.

If we assume that a tire consists of a row of elastic bristles that touches the road plane and can deflect in a direction parallel to the road surface as described in [18], the tire lateral force (f_y) and tire aligning torque (τ_a) can be modeled by simple equations, e.g. brush model. Tire brush model is proper for estimation or control purposes because it has fewer parameters compared with many other tire models [19]-[21].

The pure-slip lateral tire force model is

$$f_y = \begin{cases} -3\mu F_z \gamma \left\{ 1 - |\gamma| + \frac{1}{3}(\gamma)^2 \right\}, & \text{for } |\alpha| \leq \alpha_{sl} \\ -\mu F_z \text{sgn}(\alpha), & \text{for } |\alpha| > \alpha_{sl} \end{cases}, \quad (3)$$

and the tire self-aligning torque model is

$$\tau_a = \begin{cases} \mu F_z t \gamma (1 - 3|\gamma|)^3, & \text{for } |\alpha| \leq \alpha_{sl} \\ 0, & \text{for } |\alpha| > \alpha_{sl} \end{cases}, \quad (4)$$

where $\gamma = \theta_y \sigma_y$, $\alpha_{sl} = \tan^{-1}(1/\theta_y)$, $\theta_y = C_{af}/(3\mu F_z)$, $\sigma_y = \tan(\alpha)$, t is the half of tire contact length, α is the tire slip angle, μ is the tire-road frictional coefficient, F_z is the tire normal force, and C_{af} is the cornering stiffness of the tire.

C. Steering System Model

The steering system shown in Fig. 3 is described by the following differential equation:

$$J_{eff} \ddot{\delta} + b_{eff} \dot{\delta} = \tau_a + \tau_s + \tau_m - \tau_f, \quad (5)$$

where J_{eff} is the effective moment of inertia and b_{eff} is the effective damping of the steering system at the road wheels. τ_a , τ_s , τ_m , and τ_f represent the self-aligning torque, steering wheel torque, motor torque, and frictional torque at the road wheel, respectively.

We can measure τ_s with a torque sensor installed at steering column and can predetermine τ_f from a Coulomb friction model. The motor torque, τ_m , is expressed as the following equation:

$$\tau_m = K_m i_{eff}, \quad (6)$$

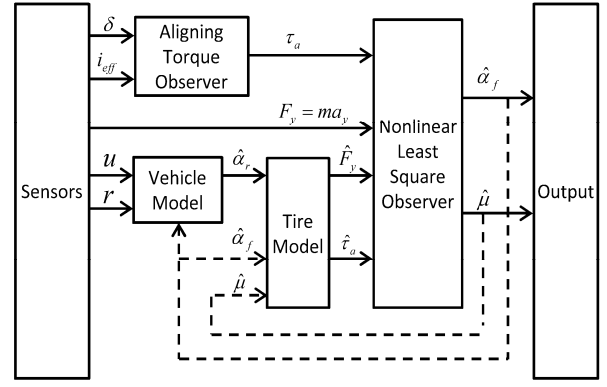


Fig. 4. Block diagram of estimation process

where K_m is the motor constant and i_{eff} is the effective motor current considering the gear ratio and the efficiency.

III. TIRE ALIGNING TORQUE OBSERVER

It is difficult to acquire tire aligning torque data in traditional passenger cars. However, if the car has EPAS or AFS, then steering wheel angle, steering wheel torque, and assisting motor torque are available. Thus it is possible to get the tire aligning torque indirectly using (3), (4), and the signals, through a linear steering system model, as shown (7) and (8). The states are steering angle, steering angle speed, and tire aligning torque. The measurement is steering wheel angle. Finally, the system inputs are effective motor current (i_{eff}) and steering wheel torque (τ_s). We assume the self-aligning torque is disturbance as shown in [3].

$$\begin{aligned} \dot{x} &= Ax + Bu, \\ y &= Cx, \\ x &= [\delta, \dot{\delta}, \tau_a]^T, u = [i_{eff}, \tau_s]^T, \\ A &= \begin{bmatrix} 0 & 1 & 0 \\ 0 & -\frac{b_{eff}}{J_{eff}} & \frac{1}{J_{eff}} \\ 0 & 0 & 0 \end{bmatrix}, B = \begin{bmatrix} 0 & 0 \\ \frac{K_m}{J_{eff}} & \frac{1}{J_{eff}} \\ 0 & 0 \end{bmatrix}, \\ C &= [1 \ 0 \ 0]. \end{aligned} \quad (7)$$

We constructed a Luenberger observer based on the linear system. By selecting an appropriate observer gain L , we can ensure asymptotic convergence of the estimation error.

$$\begin{aligned} \dot{\hat{x}} &= (A - LC)\hat{x} + Bu + Ly, \\ \hat{\tau}_a &= [0 \ 0 \ 1]\hat{x}. \end{aligned} \quad (8)$$

IV. MAXIMUM TORQUE METHOD

As the friction coefficient between tire and road changes, a tire aligning torque curve, as well as the peak point of the

curve vary. Therefore, we can detect the frictional coefficient if the peak aligning torque is measured. The relationship between frictional coefficient (μ) and the peak value is found by calculating the extremum of aligning torque, ignoring sign of τ_a and sign of σ_y for convenience of calculation:

$$\frac{\partial \tau_a}{\partial \sigma_y} = \mu F_z c \theta_y (1 - 4\theta_y \sigma_y)(1 - \theta_y \sigma_y)^2 = 0 \quad (9)$$

There are two extrema when $\sigma_y = 1/(4\theta_y)$ and $\sigma_y = 1/\theta_y$. The aligning curve reaches a peak point in the first case and the curve returns to the zero in the second case. From the definition of σ_y and θ_y , we have two equations.

$$\begin{aligned} \sigma_{y,peak} &= \tan(\alpha_{peak}) = 1/(4\theta_y) = 3\mu F_z / (4C_{\alpha f}), \\ \Rightarrow \mu &= \frac{\tan(\alpha_{peak}) \cdot 4C_{\alpha f}}{3F_z}, \end{aligned} \quad (10)$$

$$\begin{aligned} \tau_{a,peak} &= \tau_a(\sigma_y = 1/(4\theta_y)) = \frac{27}{256} \mu F_z c, \\ \Rightarrow \mu &= \frac{256}{27} \frac{\tau_{a,peak}}{F_z c}. \end{aligned} \quad (11)$$

These two equations tell us that if we know the tire slip angle or the aligning torque when the curve reaches the peak point we can calculate the frictional coefficient directly. Eq.(11) is more useful than (10) because tire slip angle is difficult to acquire.

The problem of this method is that detecting the peak point is possible only when (i) lateral excitation is strong, and (ii) the measurement data batch size is large to include the peak aligning torque value. However this method is still valuable in that, if we have a batch of aligning torque data, we can calculate the lower bound of frictional coefficient by detecting maximum value among the aligning torque data as follows:

$$\mu_{lower\ bound} = \frac{256}{27} \frac{\tau_{a,max}}{F_z c}, \quad \tau_{a,max} = \max_{\tau \in [t-t_h, t]} (\tau_a(\tau)). \quad (12)$$

V. NONLINEAR LEAST SQUARE METHOD

A. Basic Equations

Hsu [11] used nonlinear least squares to identify frictional coefficient. He only used self-aligning torque with GPS-based sideslip measurements. In this section, we introduce a nonlinear least square method that uses both vehicle model and tire model. The basic information for the method is the vehicle lateral acceleration (from accelerometer) and the self-aligning torque, obtained using the tire aligning torque observer described in the previous section. Vehicle lateral force is the sum of lateral directional tire forces, as described in (1). We can easily calculate the

vehicle lateral force by multiplying lateral acceleration, a_y , and the vehicle mass, m :

$$ma_y = f_y(\alpha_r, \mu) \cos \delta + f_y(\alpha_f, \mu), \quad (13)$$

where f_y is a tire lateral force, which is a function of tire slip angle and frictional coefficient, as described in (3). Rear tire slip angle α_r is determined by (2) if front tire slip angle α_f is known and u, r, δ are measured. As a result, the left side of (13) is determined by measurement and the right side is a function of α_f and μ .

Tire self-aligning torque is a function of α_f and μ , as expressed in (4):

$$\tau_a = \tau_a(\alpha_f, \mu), \quad (14)$$

and the tire self-aligning torque can also be determined by the aligning torque observer. Therefore, we have the second relationship:

$$\tau_{a,obs} = \tau_a(\alpha_f, \mu), \quad (15)$$

where $\tau_{a,obs}$ is the observed tire self aligning torque. Finally, we have two unknowns, α_f and μ , and two equations, (13) and (15) so that we are theoretically able to determine two unknowns. Nevertheless, the two equations are nonlinear so it is difficult to solve the equations directly. Nonlinear least square methods are used to find the best candidates of the unknowns ensuring the smallest error in the sense of least square.

B. Solving with single datum

The process of solving the two nonlinear equations is the same as finding the optimal of α_f and μ which minimize the errors between the measured force/torque and the calculated force/torque using tire model.

$$\min_{\alpha_f, \mu} |F_y - F_{y,measure}|, \quad \min_{\alpha_f, \mu} |\tau_a - \tau_{a,obs}| \quad (16)$$

We introduce a blended cost function as follows.

$$J(x) = \frac{1}{2} \left(\left| \hat{F}_y(x) - \bar{F}_y \right|^2 + \left| \hat{\tau}_a(x) - \bar{\tau}_a \right|^2 \right), \quad (17)$$

where

$$\begin{aligned} x &= [\alpha, \mu]^T, \\ \hat{F}_y &= \frac{2}{mg} (f_{yf}(\alpha_f, \mu) \cos \delta + f_{yr}(\alpha_r, \mu)), \\ \hat{F}_y &= \frac{2}{mg} ma_y, \quad \hat{\tau}_a = \frac{1024}{27mgc} \tau(\alpha_f, \mu), \quad \bar{\tau}_a = \frac{1024}{27mgc} \tau_{a,obs}. \end{aligned}$$

The force terms and torque terms are normalized to consider equivalent effects on the cost function.

C. Solving with multiple data

Even though we can solve the nonlinear equation described in the previous section, the result will be vulnerable to measurement noise or observer error in a_y and $\tau_{a,obs}$.

To be robust against the noise and model uncertainties, we use a nonlinear least square method with n length of measurement data. The cost function to be minimized is

$$J(x) = \frac{1}{2} \left(\left| \hat{F}_y(x) - \bar{F}_y \right|^2 + w \left| \hat{\tau}_a(x) - \bar{\tau}_a \right|^2 \right), \quad (18)$$

where

w : weighting factor,

$$x = [\alpha_{f1}, \alpha_{f2}, \dots, \alpha_{fn}, \mu]^T,$$

$$\hat{F}_y = [F_y(1), F_y(2), \dots, F_y(n)]^T,$$

$$\bar{F}_y = [ma_{y1}, ma_{y2}, \dots, ma_{yn}]^T,$$

$$F_y(k) = f_{yf}(\alpha_{fk}, \mu) \cos \delta_k + f_{yr}(\alpha_{rk}, \mu),$$

$$\hat{\tau}_a = [\tau(\alpha_{f1}, \mu), \tau(\alpha_{f2}, \mu), \dots, \tau(\alpha_{fn}, \mu)]^T,$$

$$\bar{\tau}_a = [\tau_{a,obs1}, \tau_{a,obs2}, \dots, \tau_{a,obsn}]^T.$$

We assume μ is constant among the data set whereas slip angles are not constant. As a result, we have $n+1$ unknowns (n α_f s and a μ) and $2n$ equations (n force equations and n torque equations). These nonlinear equations are over-determined and we obtain more robust results.

D. Initial Value of Nonlinear Least Squares

Nonlinear least square method starts from an initial guess and search for better results iteratively. Therefore, it is not guaranteed to converge to the global optimum and the results depend on the initial guess. Choice of appropriate initial α_f and μ in the each time step is important. The optimal values of the previous time step are generally used as the initial values. Indeed, if we offer a more probable candidate for the initial values then we can reduce iteration time and improve accuracy. Also, if there are several local minima in the cost function, offering a plausible initial value is very helpful. The most plausible candidates for the parameters can be projected with their dynamics. We can obtain the dynamics of α_f from (2) and dynamics of μ by assuming it is constant.

$$\dot{\alpha}_f = \left(\frac{1}{mu} + \frac{a^2}{I_z u} \right) F_{yf} + \left(\frac{1}{mu} - \frac{ab}{I_z u} \right) F_{yr} - r - \dot{\delta}, \quad (19)$$

$$\dot{\mu} = 0. \quad (20)$$

VI. SIMULATION RESULTS

We verify the performance of the two algorithms with Carsim with three levels of frictional coefficient with a vehicle speed of 60 km/h and a steer input of 0.25Hz sine

wave with a magnitude of 0.04 rad.

Maximum Torque method shows poor quality in estimating frictional coefficient and does not estimate slip angle. However, as mentioned previously, the frictional coefficient estimated by the maximum torque method is the low bound of real frictional coefficient, in fact, the coefficient estimated by the maximum torque method (the green lines in Fig. 5, Fig. 6, and Fig. 7) is always under the real coefficient (yellow lines).

Even though the maximum torque method is not useful to estimate the coefficient accurately, it can provide the lower limit for the frictional coefficient for other estimators. In fact, the other methods considered in this paper use this underestimated frictional coefficient as the lower bound. As shown Figs. 5-7, friction coefficients estimated by the other methods are always higher than that of maximum torque method.

We use a damped Gauss-Newton method to solve the nonlinear problem. The required computational time for multiple data approach is 0.015sec, using the hardware Intel Core2 Duo CPU at 2GHz and the software Matlab 2007a. Both nonlinear least square methods show acceptable estimation result when the real friction coefficient is high (1.0). However nonlinear least square method with single datum underestimates the coefficient at $\mu = 0.5$, whereas nonlinear least square method with multiple data shows better estimation results. When the friction coefficient is low (0.2), nonlinear least square method with single datum present completely an incorrect result because it fails to find the global minimum. This problem can happen in any nonlinear least square method, but if we have enough information and appropriate excitation, then the possibility of reaching the global minimum increases. In the verification, the length of a data set is 40, equivalent to a time horizon of 0.8 sec. In the process of nonlinear least square method with 40 data, the estimator tries to find 40 different optimal slip angles and one frictional coefficient with 80 given conditions, so the estimated frictional coefficient is as averaged value within the

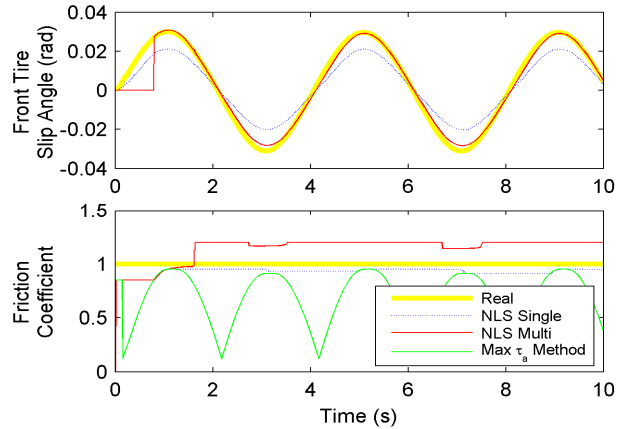


Fig. 5. Simulation result when frictional coefficient is 1.0. NLS Single is Nonlinear least square method with single datum, NLS Multi is Nonlinear least square method with several data, and Max τ_a Method is Maximum torque method.

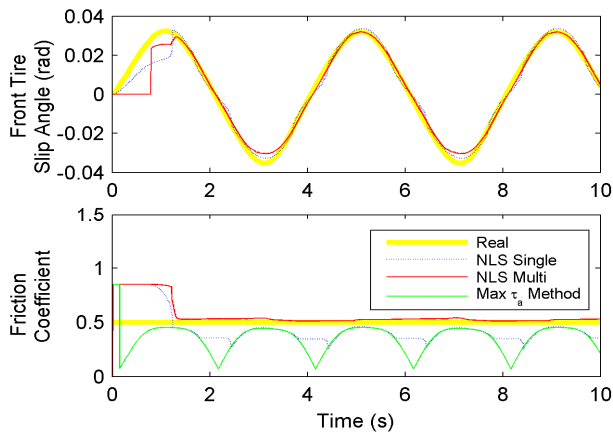


Fig. 6. Simulation result when frictional coefficient is 0.5.

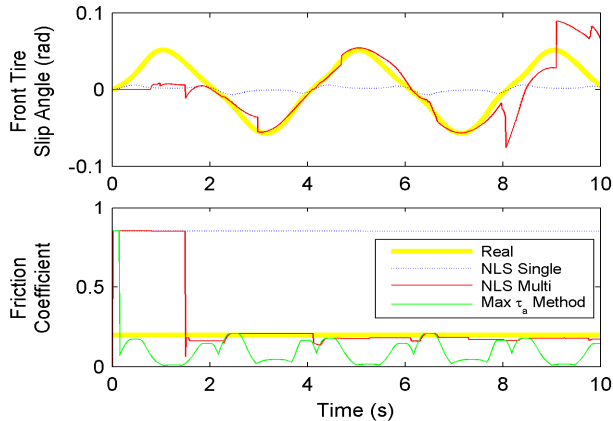


Fig. 7. Simulation result when frictional coefficient is 0.2.

past 0.8 seconds. As a result, nonlinear least square method with several data is more stable than with single datum.

VII. CONCLUSION

This paper presents three estimators for the coefficient of friction. Maximum torque method always underestimates frictional coefficient, but it does not require tire slip angle and it is valuable because provides a lower bound for frictional coefficient estimation. Nonlinear least square method with single datum shows acceptable performance on high friction surface, but it fails on low friction roads. Nonlinear least square method with multiple data points shows the best performance and stable estimation, but its performance is not guaranteed. Better performance is achieved by increasing the size of the data set and guessing good initial values. However, using a long data set induces delay and increases computation load. The optimal length of the data set was determined empirically.

Further study on robustness of the observers against uncertainties and development of effectively fast nonlinear least square algorithm for calculation time reduction will be conducted.

REFERENCES

- [1] U. Eichhorn and J. Roth, "Prediction and monitoring of tyre/road friction," in *Proc. FISITA 24th Congress: Safety, the Vehicle, and the Road, Tech. Paper*, London, U.K., 1992, vol. 2, pp. 67–74.
- [2] M. Ito *et al.*, "Estimation of road surface conditions using wheel speed behavior," in *Proc. Int. symp. Advanced Vehicle Control*, Tsukuba, Japan, 1994, pp. 533–538.
- [3] C. Pal *et al.*, "Application of neural networks in real time identification of dynamic structural response and prediction of road-friction coefficient from steady state automobile response," in *Proc. Int. symp. Advanced Vehicle Control 1994*, Tsukuba, Japan, 1994, pp. 527–532.
- [4] W. R. Pasterkamp and H. B. Pacejka, "The tyre as a sensor to estimate friction," *Vehicle System Dynamics*, vol. 27, no. 5, pp. 409–422, Jun. 1997.
- [5] F. Gustafsson, "Monitoring tire-road friction using the wheel slip," *IEEE Control Syst. Mag.*, vol. 18, no. 4, pp. 42–49, Aug. 1998.
- [6] C. Liu and H. Peng, "Road friction coefficient estimation for vehicle path prediction," *Vehicle System Dynamics*, vol. 25, suppl. pp. 413–425, Jan. 1996.
- [7] J. Hahn *et al.*, "GPS-based real-time identification of tire-road friction coefficient," *IEEE Trans. Control Syst. Technol.*, vol. 10, no. 3, pp. 331–343, May. 2002.
- [8] C. Sierra *et al.*, "Cornering stiffness estimation based on vehicle lateral dynamics," *Vehicle System Dynamics*, vol. 44, suppl., pp. 24–38, Jan. 2006.
- [9] Y. Yasui *et al.*, "Estimation of lateral grip margin based on self-aligning torque for vehicle dynamics enhancement," in *SAE 2004 World Congress & Exhibition*, Detroit, USA, 2004, paper no. 2004-01-1070.
- [10] E. Ono, "Estimation and control of vehicle dynamics for active safety," *R&D Review of Toyota CRDL*, vol. 40, no. 4, pp. 1–6, Sep. 2005.
- [11] E. Ono *et al.*, "Estimation of tire friction circle and vehicle dynamics integrated control for four-wheel distributed steering and four-wheel distributed traction/braking systems," *R&D Review of Toyota CRDL*, vol. 40, no. 4, pp. 7–13, Sep. 2005.
- [12] T. Umeno, "Detection of tire lateral force based on a resolver mechanism," *R&D Review of Toyota CRDL*, vol. 40, no. 4, pp. 14–19, Sep. 2005.
- [13] Y. Hsu and J. C. Gerdes, "A feel for the road: a method to estimate tire parameters using steering torque," in *Proc. Int. symp. Advanced Vehicle Control*, Taipei, Taiwan, 2006, pp. 1–6.
- [14] Y. Hsu *et al.*, "A method to estimate the friction coefficient and tire slip angle using steering torque," in *Proc. 2006 ASME Int. Mech. Eng. Congr. Expo.*, Chicago, Illinois, 2006, pp. 1–10.
- [15] F. Holzmann *et al.*, "Predictive estimation of the road-tire friction coefficient," in *Proc. 2006 IEEE Int. Conf. Control Applicat.*, Munich, Germany, 2006, pp. 885–890.
- [16] Y. Sato *et al.*, "Study on recognition method for road friction condition," *JSAE Trans.*, vol. 38, no. 2, pp. 51–56, Mar. 2007.
- [17] M. Yamada, "Road surface condition detection technique based on image taken by camera attached to vehicle rearview mirror," *Review of Automotive Engineering*, pp. 163–168, Apr. 2005.
- [18] H. B. Pacejka, "Tyre brush model" in *Tyre and Vehicle Dynamics*, 2nd ed. Oxford, U.K., Elsevier, 2005, pp. 93–134.
- [19] H. B. Pacejka, "The tread simulation model" in *Tyre and Vehicle Dynamics*, 2nd ed. Oxford, U.K., Elsevier, 2005, pp. 134–147.
- [20] H. B. Pacejka, "Semi-empirical tyre models" in *Tyre and Vehicle Dynamics*, 2nd ed. Oxford, U.K., Elsevier, 2005, pp. 156–215.
- [21] H. B. Pacejka, "Non-steady-state out-of-plane string-based tyre models" in *Tyre and Vehicle Dynamics*, 2nd ed. Oxford, U.K., Elsevier, 2005, pp. 216–294.